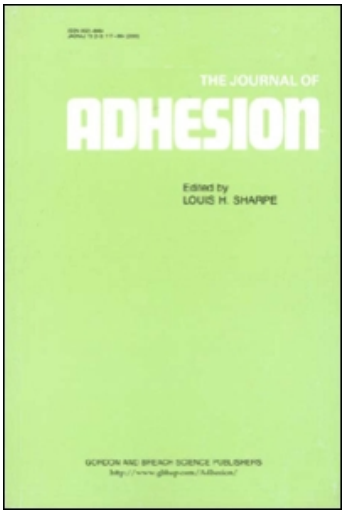

The Journal of Adhesion
Publication details, including instructions for authors and subscription information:
http://www.informaworld.com/smpp/title~content=t713453635

Dissipative Processes in Interfacial Failure

M. J. Napolitano[a]; A. Moet[a]
[a] Department of Macromolecular Science, Case Western Reserve University Cleveland, Ohio, USA

To cite this Article Napolitano, M. J. and Moet, A.(1991) 'Dissipative Processes in Interfacial Failure', The Journal of Adhesion, 33: 3, 149 — 167
To link to this Article: DOI: 10.1080/00218469108030424
URL: http://dx.doi.org/10.1080/00218469108030424

J. Adhesion, 1991, Vol. 33, pp. 149–167
Reprints available directly from the publisher
Photocopying permitted by license only

Printed in the United Kingdom

Dissipative Processes in Interfacial Failure

M. J. NAPOLITANO and A. MOET

Department of Macromolecular Science, Case Western Reserve University Cleveland, Ohio 44106-2699, USA

(Received January 29, 1990; in final form August 28, 1990)

An investigation of the failure behavior of pressure sensitive adhesive tape was performed utilizing the constrained blister test. The constrained blister test was designed to measure the energy of interfacial adhesion of thin polymeric coatings. A constant energy of interfacial adhesion of $1.8\,J/m^2$ was determined for a rubber based pressure sensitive adhesive on a copper substrate. An active zone was visualized through the transparent backing. The deformation within the active zone was found to consist of cavitation and deformation of ligaments. Fracture of the ligaments causes the detachment front to advance. It was proposed that the rate of energy dissipation, $\dot{D}$, reflects the resistance of the bond to time dependent deformation, and therefore dictates the lifetime for this particular specimen geometry. A direct relationship was established between lifetime and the inverse of the rate of energy dissipation in the active zone, $\dot{D}$.

KEY WORDS Adhesion; constrained blister; dissipation; pressure sensitive adhesive; fracture energy; lifetime.

INTRODUCTION

Long term performance of an adhesive bond, like other engineering structures, is controlled not only by its fracture energy but also by the rate at which energy is dissipated within the bond in the resistance to service loads. Both ought to be fundamentally parameterized for successful design and accurate prediction of performance. In spite of the generally accepted principle that improved performance of adhesive bonds rests on their enhanced dissipative character, toughened epoxies represent a bright example,[1] recent research on adhesion measurements[2–15] has been limited to techniques to evaluate the fracture energy. Meager attention is directed toward developing a methodology to parameterize and evaluate the dissipative character of adhesives in conjunction with their strength. Nevertheless, it has been shown that energy dissipation plays an important role in the strength of adhesive bonds.[16–18]

This paper presents an analysis of the exploration of the nature of dissipative mechanisms in the "adhesive" failure of a transparent tape, utilizing the constrained blister test.[19–21] The associated formalism developed by Moet *et al.*[20] is

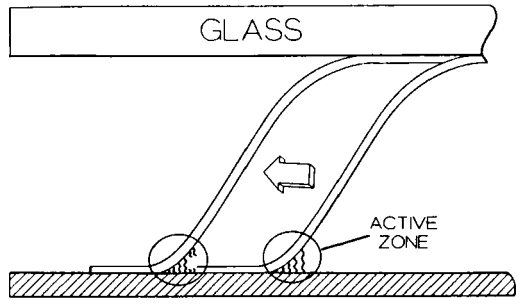

FIGURE 1 Schematic of propagation of the constrained blister. Growth is accompanied by the formation of an active zone ahead of the peel front and before the new surface has been created.

employed to evaluate the energy of interfacial adhesion and a phenomenological coefficient related to dissipative processes at different loading conditions.

The detachment process in the constrained blister configuration consists of steady state propagation of a detachment front. The detachment front is envisioned to be preceded by a zone of damage (active zone) in which dissipative processes accumulate, leading to failure (Figure 1).

EXPERIMENTAL

A schematic of a cross section of the constrained blister apparatus is presented in Figure 2. Commercial nitrogen was used as a pressurizing medium. The separation between the constraining glass plate and the tape was controlled by metallic spacers. Blister propagation was monitored with a video camera and recorded with a time lapsed video recorder. The active zone geometry was examined in a separate experiment with a Nikon optical microscope.

A commercial pressure sensitive adhesive tape from 3M Corporation was used in this study (Catalog #483). The tape was composed of a transparent polyethylene backing (100 μm) with a rubber-based adhesive layer (25 μm). The substrate tested was a copper plate with a 3.2 mm pressure inlet hole. The surface

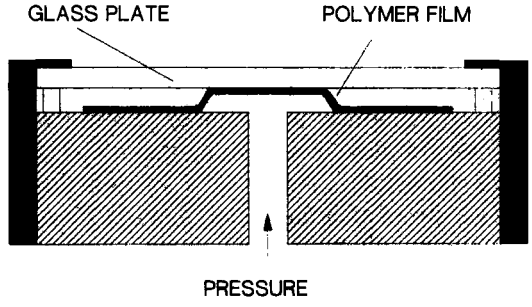

FIGURE 2 Schematic of the constrained blister testing apparatus.

of the substrate was prepared through a series of polishing and washing steps. Sandpaper of 200, 400, and 600 grit was successively used. A final polish with 0.3 μm alumina was performed. The polished substrates were then rinsed in acetone, placed in a 10% HCl solution for 10 minutes, then rinsed in deionized water.[22] The substrate was then blown dry with nitrogen. The tape was tested over a range of pressures and spacer heights. All tests were performed at room temperature.

In order to assure reproducibility in the testing of the pressure sensitive adhesive tape, the effect of dwell time and application load were investigated. We have found that an improper dwell time and/or application pressure lead to a high degree of irreproducibility between runs at equivalent conditions. In addition, asymmetric growth of the blister is usually observed below a certain critical dwell time and application load. Dwell time is defined as the time between applying the adhesive film to the copper surface and the actual testing. In Figure 3, the effect of dwell time on the rate of radial propagation (dr/dt) is presented for samples tested at a pressure of 0.28 MPa and a spacer height of 0.69 mm. In the first 24 hours of dwell time, a rapid increase in the rate of radial propagation is observed. Dwell time of 24 hrs and above produces an asymptotic radial propagation rate. Therefore, a dwell time of 24 hrs was chosen in order to reduce the variations in the rate of radial propagation.

Similarly, the effect of application load was investigated. A constant load was achieved by applying dead weights to the film surface after depositing the film. A rubber mat (3.2 mm thick) was used to distribute the load over a substrate area of

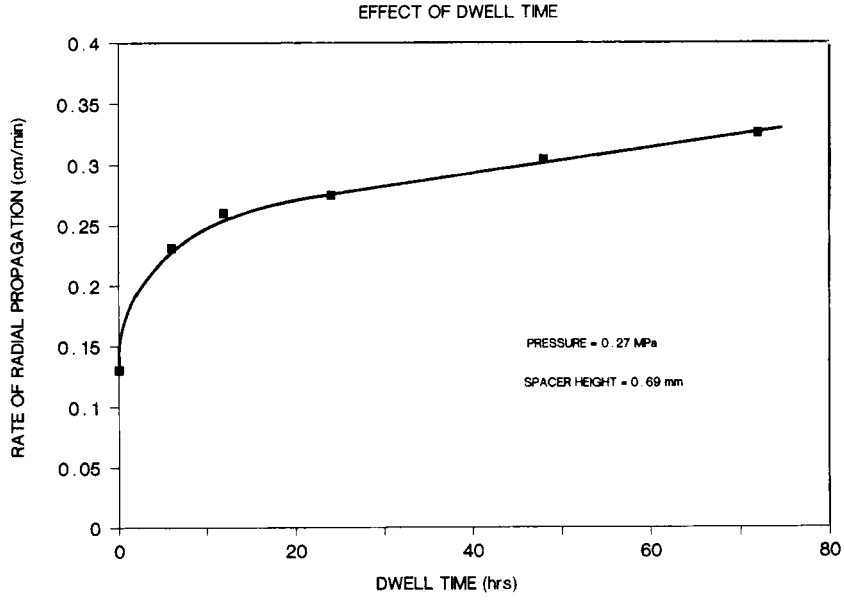

FIGURE 3 Effect of dwell time on the rate of radial propagation for tape tested at 0.27 MPa pressure and spacer height of 0.69 mm.

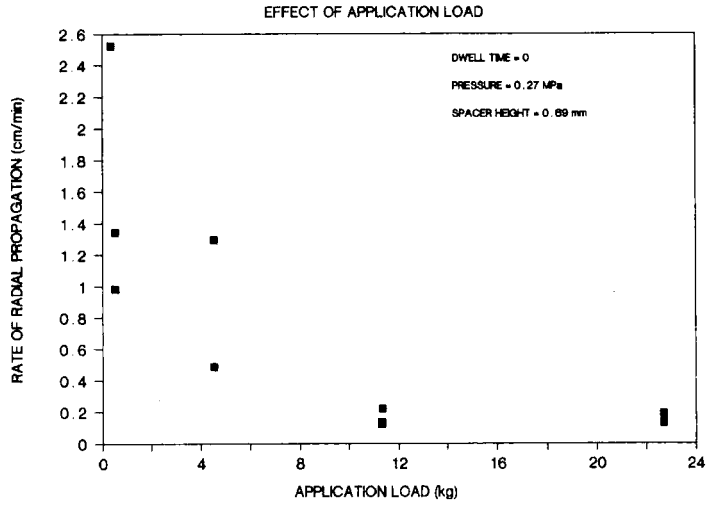

FIGURE 4 Effect of application load on the rate of radial propagation for tape tested at 0.27 MPa pressure and a spacer height of 0.69 mm.

9.7 cm^2. In Figure 4, the effect of application load on the rate of radial propagation is presented. At low loads, there is a high degree of scatter in the rate data. At higher loads, the scatter is significantly reduced and the propagation rate approaches an asymptotic value of 1.6 cm/min. Based on the above results, an application load of 23 kilograms was used in all tests.

RESULTS

Blister propagation

In Figure 5, photographs taken from a video monitor of the developmental stages of the constrained blister are presented for a tape tested at 0.41 MPa and a spacer height of 0.69 mm. Upon application of pressure, a blister rapidly forms and expands (Figure 5b). Further growth of the blister causes the film to come into contact with the glass plate (Figure 5c). In Micrograph 5c, R_1 denotes the detached radius and R_2, the constrained radius. From the micrographs it is evident that the blister growth has two distinct stages. The first stage is the growth of the blister until contact with the plate is made. When contact has been made, the second stage begins and radial propagation of the constrained blister is observed. Blister propagation occurs when fracture of ligaments causes the detachment front to advance (see Figure 6).

Kinetics

A representative radial propagation curve for both the detached and constrained radii are presented in Figure 7. The radius at time zero was taken as the radius of

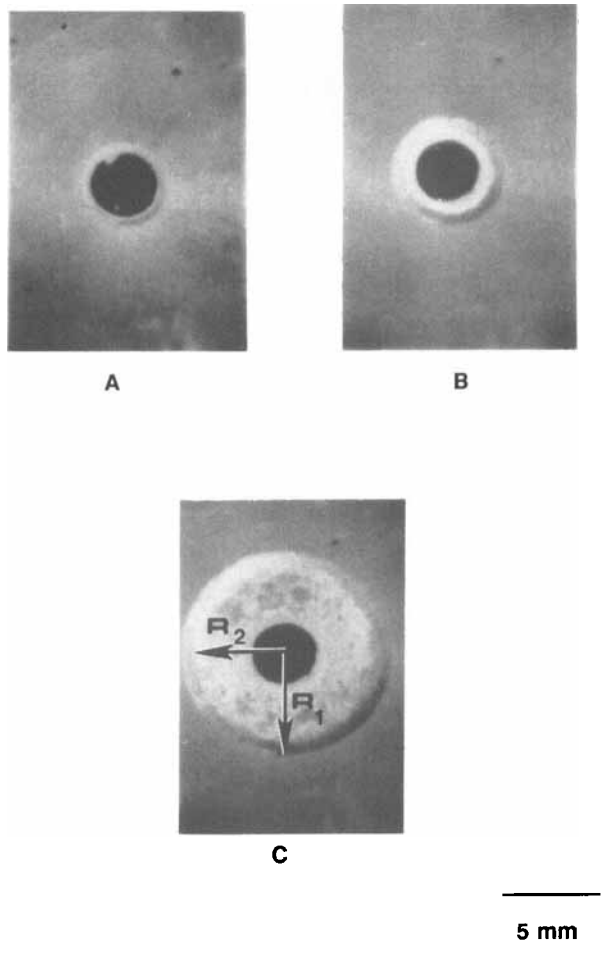

FIGURE 5 Photographs taken off a video monitor showing blister development as a function of time for a PSA tape under an applied pressure of 0.41 MPa and a spacer height of 0.69 mm at: A) 2 sec; B) 5 sec; and C) 24 sec.

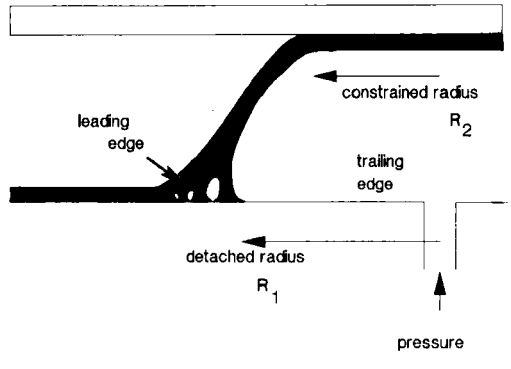

FIGURE 6 Schematic of constrained blister propagation. R_1 is the detached radius; R_2, the constrained radius.

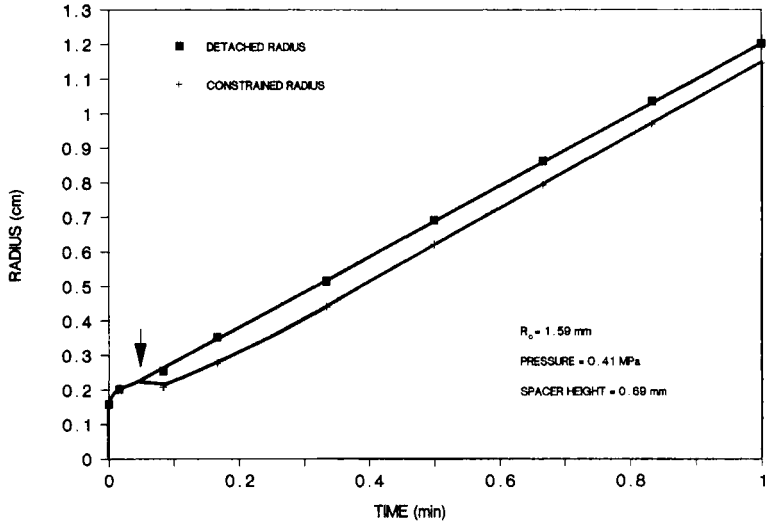

FIGURE 7 Detached and constrained radii *versus* time for a tape tested at 0.41 MPa pressure and spacer height of 0.69 mm.

the pressure inlet hole. One observes an initiation region (marked by the arrow), along with a region of linear growth in radius with time. Similarly, Dillard *et al.* observed that the debonding radius increases linearly with time in the case of a PSA tape with a polyester backing and a rubber-based adhesive.[21] This linearity in the radius *versus* time behavior was observed for all samples tested.

In Table I, the various combinations of pressure and height experimentally investigated are presented along with the rate of blister area propagation (dA/dt). No strong correlation exists between rate of blister area propagation and the variables of height or pressure alone. However, it was seen that the rate of blister

TABLE I
Experimental combinations of applied pressure and spacer height with corresponding rates of blister area propagation data

Pressure (Pa)	Height (mm)	PH (J/sq m)	dA/dt (sq m/min)
34,474	0.254	9	5.02E-09
68,947	0.254	18	5.31E-08
68,947	0.686	47	1.16E-07
137,895	0.381	53	7.07E-08
137,895	0.686	95	3.48E-07
275,789	0.381	105	8.65E-07
275,789	0.508	140	3.03E-06
206,842	0.686	142	1.97E-06
275,789	0.686	189	2.37E-05
275,789	0.762	210	2.73E-05
344,737	0.686	236	4.63E-05
413,684	0.686	284	3.33E-04

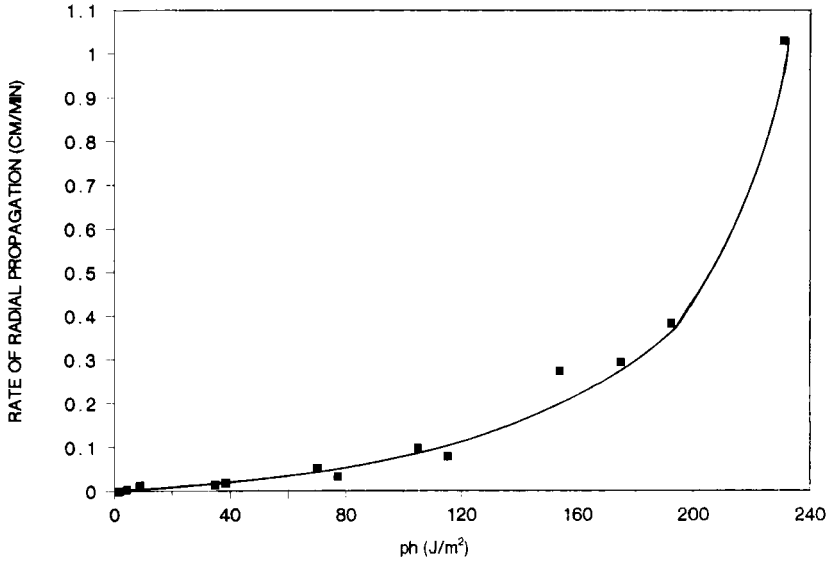

FIGURE 8 Rate of blister propagation *versus ph*.

area propagation increased with the product of pressure and height (see Figure 8). Indeed, Dillard *et al.* have shown that the strain energy release rate for the constrained blister geometry is related to the product of the pressure and blister height.[21] This reaffirms the notion that the product, ph, is indeed a characteristic variable of constrained blister propagation.

Active zone kinetics

The active zone length (see Figure 6) was measured using a Nikon optical microscope with a video camera attachment. In Figure 9, the active zone length is presented as a function of time for a tape tested at 0.41 MPa applied pressure and a spacer height of 0.69 mm. In the region where the blister is constrained, there is a large increase in the active zone length with time. When the blister becomes constrained, the active zone length was found to be highly dependent on the spacer height and less so on the applied pressure (Figures 10 and 11). At a constant pressure of 0.28 MPa, the active zone length was found to increase with spacer height. At a constant spacer height, an increase in the active zone length was observed with increasing pressure, but the change was less than that observed for changing spacer height while keeping pressure constant. Intuitively, one expects the height, which controls the shape of the unconstrained portion of the detached tape, to play a larger role in determining the active zone length.

Although the active zone length for a specified pressure and spacer height was found to be a constant, there is a significant increase in the active volume with redial propagation. Due to the rapid radial growth in this experiment, the active

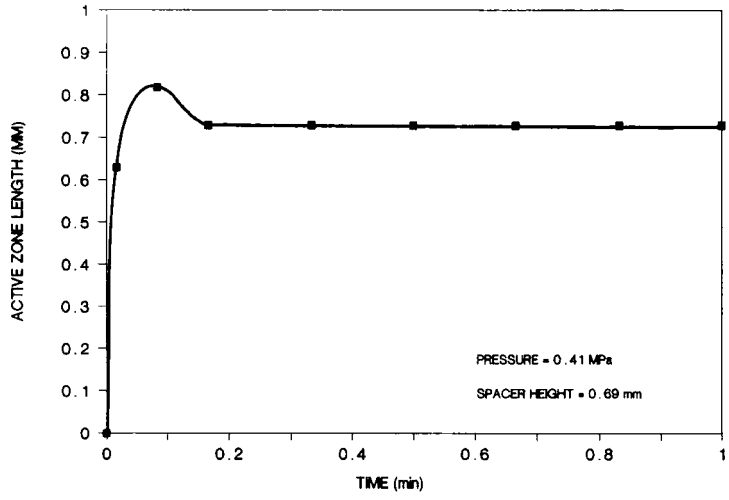

FIGURE 9 Active zone length *versus* time for tape tested at 0.41 MPa pressure and spacer height of 0.69 mm.

zone height could not be directly measured. To compute the active zone volume, the active zone height was approximated as the thickness of the adhesive layer (25 μm). A representative plot of the computed active zone volume *versus* time is presented in Figure 12 for a tape tested at a pressure of 0.41 MPa and a spacer height of 0.69 mm. A rapid increase in active zone volume is observed during blister initiation, followed by a linear region until ultimate failure occurs.

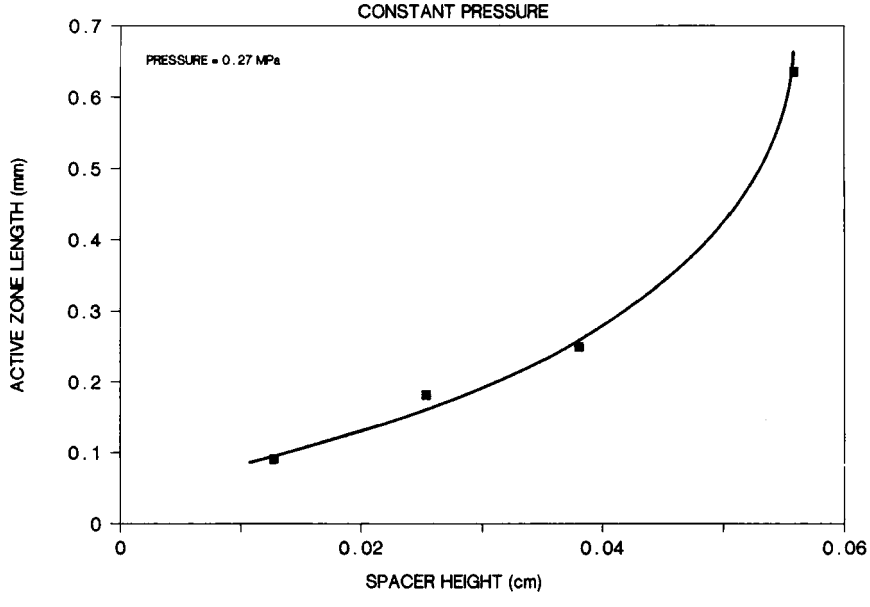

FIGURE 10 Active zone length *versus* pressure at a constant pressure.

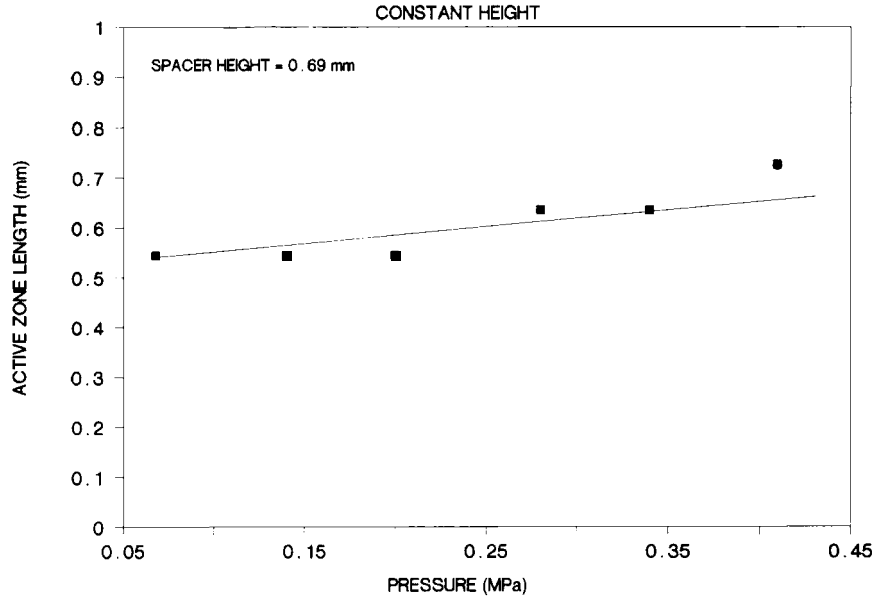

FIGURE 11 Active zone length *versus* pressure at constant spacer height.

At the front of the active zone (leading edge) cavitation takes place in the adhesive layer (Figure 13). Debonding of the adhesive layer from copper has taken place, creating isolated ligaments. As we approach the detached front, the ligaments become stretched and elongated. The ligaments then fracture and the front advances.

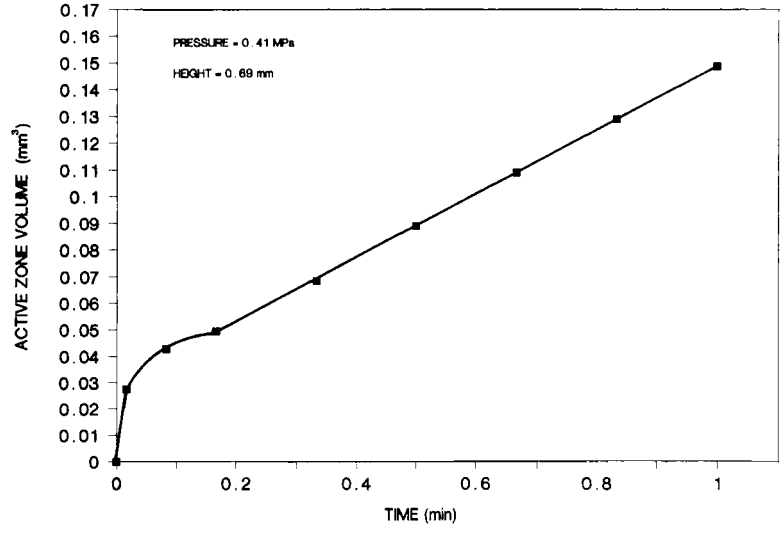

FIGURE 12 Active zone volume *versus* time for a tape tested at 0.41 MPa pressure and a spacer height of 0.69 mm.

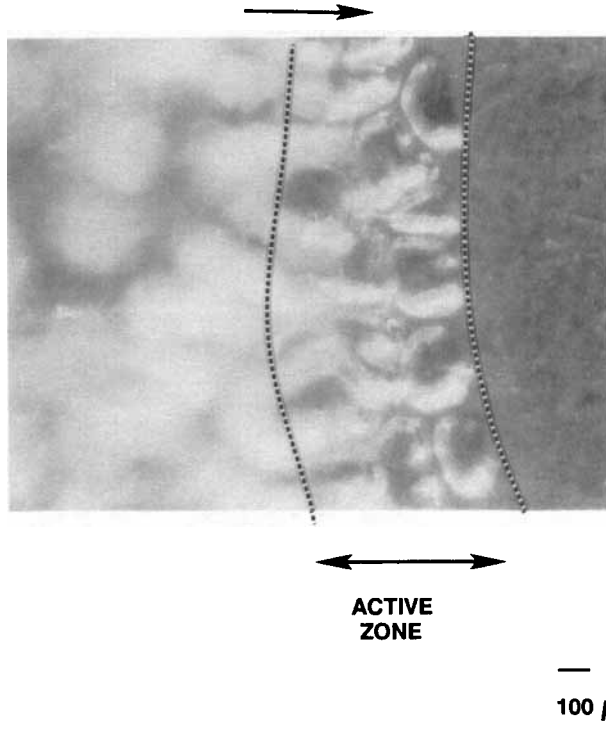

FIGURE 13 Optical micrograph of the leading edge of the active zone showing extensive cavitation.

Post failure analysis

Microscopic evaluation was performed on the adhesive and adherend surface. In Figure 14, a reflected light micrograph of the detached adhesive surface of a tape tested at a *ph* of 38.5 J/m^2 is presented. The arrow marks the direction of radial propagation. The highlighted zone in the micrograph appears to contain areas of cavitation. The cavitation streaks are elongated in the propagation direction. The area surrounding the cavitation zones resembles that of the portion of the tape placed over the pressure inlet hole (see Figure 15).

In Figure 16, a SEM micrograph of a region of tape under the pressure inlet hole shows a surface devoid of any noticeable features. The marker dots trace the edge of the pressure inlet hole. Note the presence of elongated cavitated zones past the edge of the pressure inlet hole (arrow, Figure 16). Cavitation of the adhesive layer has been previously reported for pressure sensitive adhesive tapes[23–26] and rubber adhesive joints.[16,27] A SEM micrograph taken further down the detached front (Figure 17) reveals further details of the cavitation process. Deformed ligaments are still visible within some cavities (arrow 1, Figure 17). At higher magnification, the deformed zones surrounding the cavities were found to be the site of fracture (see Figure 18). Cleavage of the ligaments takes place in the adhesive layer, not at the metal/polymer interface.

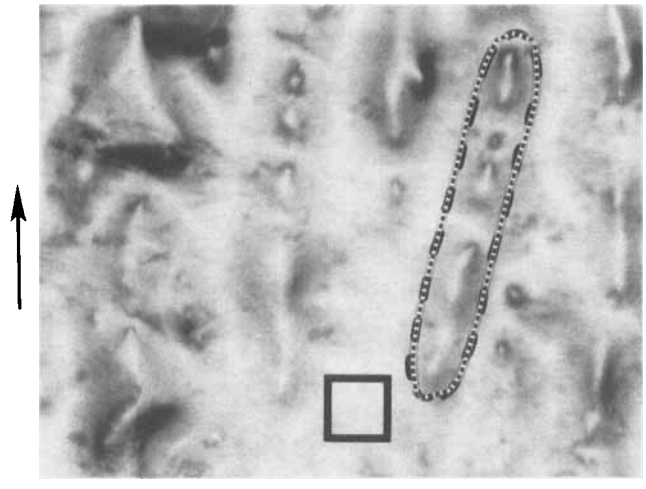

FIGURE 14 Optical micrograph of the failure surface tested at *ph* of 38.5 J/m^2. The micrographs were taken at a detached radius of 0.48 cm.

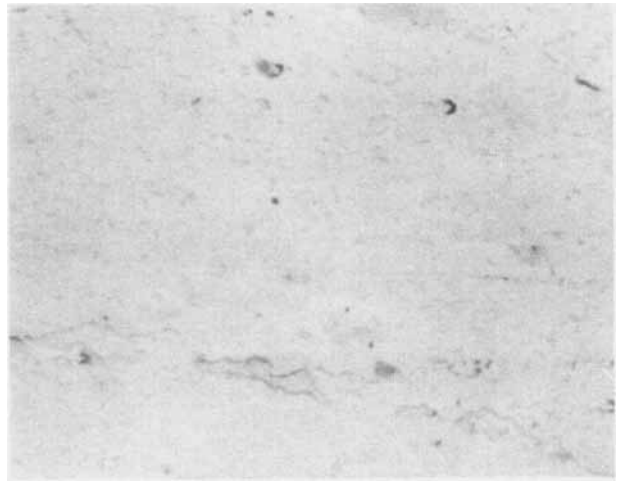

FIGURE 15 Optical micrograph of the polymer side of failure surface tested at *ph* 38.5 J/m^2. Micrograph taken from region over the pressure inlet hole.

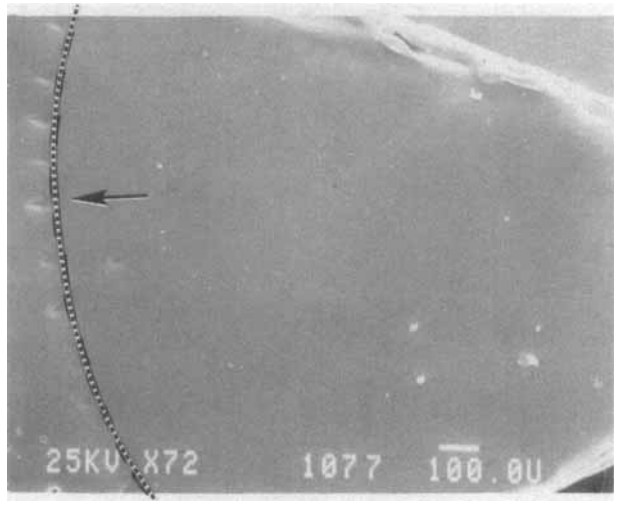

FIGURE 16 SEM micrograph of polymer side of the failure surface from region under pressure hole inlet. Dashes mark the edge of the pressure inlet hole. Arrow marks the elongated zones. $ph = 154.1\ J/m^2$.

Energy of interfacial adhesion, γ

To model blister debonding, an energy balance was previously used[20] to relate the rate of blister growth to interfacial parameters. A relationship was developed of the form:

$$\dot{A} = \dot{D}(ph - \gamma) \tag{1}$$

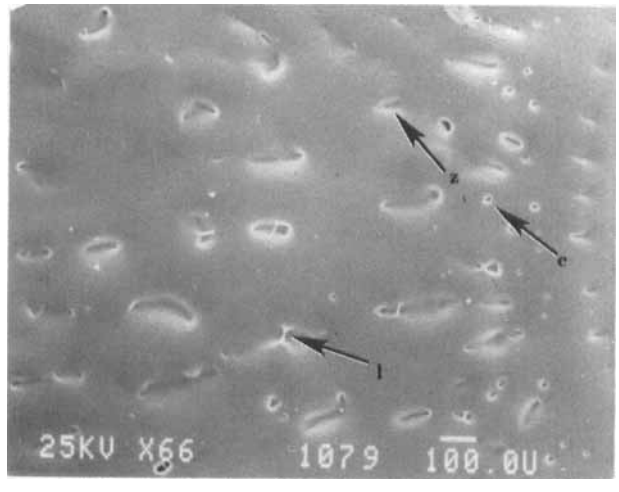

FIGURE 17 SEM micrograph of polymer side of the failure surface taken away from the failure surface. Arrows mark cavitation (c); deformed zones (z); and deformed ligaments (l). $ph = 154.1\ J/m^2$.

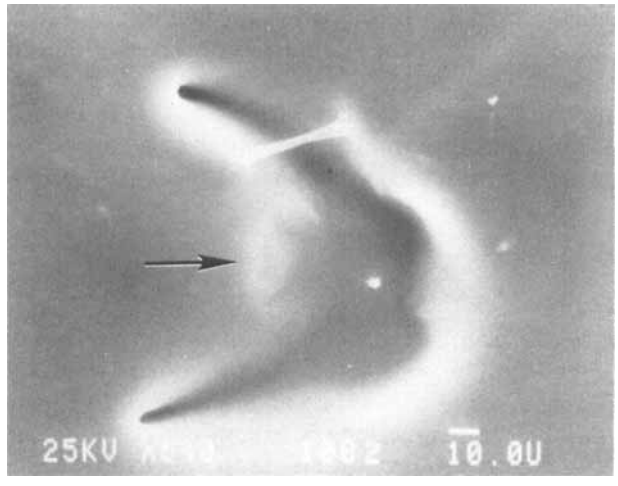

FIGURE 18 SEM micrograph of deformed zone. Arrow marks the fracture of a ligament.

where $\dot{A}$ is the rate of change in blister area, $\dot{D}$ is the rate of energy dissipation in the active zone, γ is the energy of interfacial adhesion, p is the applied pressure and h is the blister height. γ, the energy of interfacial adhesion, is a material parameter dependent only on substrate and adherend. $\dot{D}$, the rate of energy dissipated in the active zone due to irreversible processes, is dependent on both material and geometric factors. Inspection of Figure 8 shows that the rate of blister propagation approaches zero at a finite ph value. Utilizing the methodol-

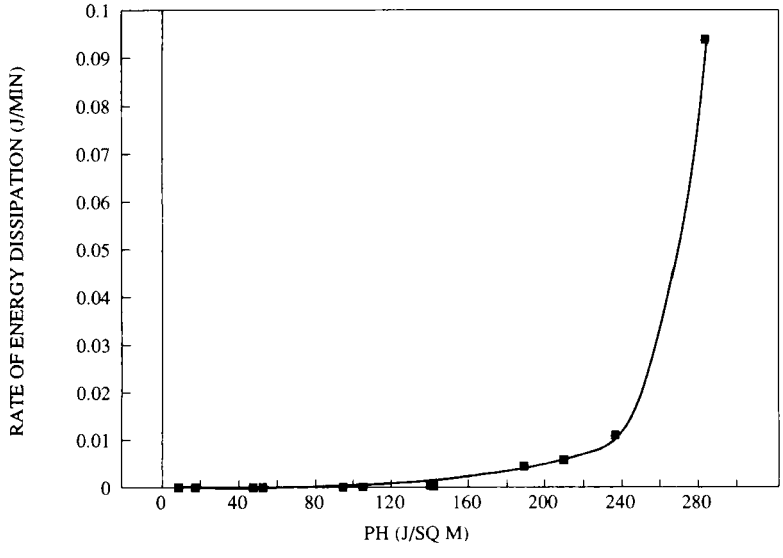

FIGURE 19 Rate of dissipation in the active zone *versus ph*.

ogy for determining γ put forth previously,[20] a value of γ of 1.8 J/m^2 was found. Below this critical *ph* value, no propagation was observed within the experimental time frame.

With γ determined, $\dot{D}$ can be calculated from Eq. (1). In Figure 19, the rate of energy dissipated in the active zone is presented as a function of *ph*. A sharp increase in $\dot{D}$ is observed with increasing *ph*.

DISCUSSION

In order to characterize adequately the behavior of an interface under load, two important parameters need be considered. As with other structural materials, the fracture energy is a measure of how strong an interface is. But just as significant is the question of durability, or how long a structure will endure under load. The fracture energy, the energy required to create the new surface, is by definition a time independent parameter. Durability, however, is related to the material's ability to dissipate energy with time. Thus "lifetime" ought to be related to the time required to initiate and propagate the active zone along the interface.

In Figure 20, lifetime (time required to initiate and propagate a constrained blister to ultimate failure) of the adhesive tape is presented as a function of *ph*, which is envisioned as a measure of the energy available to dissipative processes leading to failure. As *ph* increases, a sharp drop in the lifetime is noted. This is in direct contrast to the observed behavior of $\dot{D}$ which increases with *ph* (see Figure 19). Although $\dot{D}$ is related to many factors (film properties, text geometry, and dissipative processes), the analysis of $\dot{D}$ is consistent within a set of given

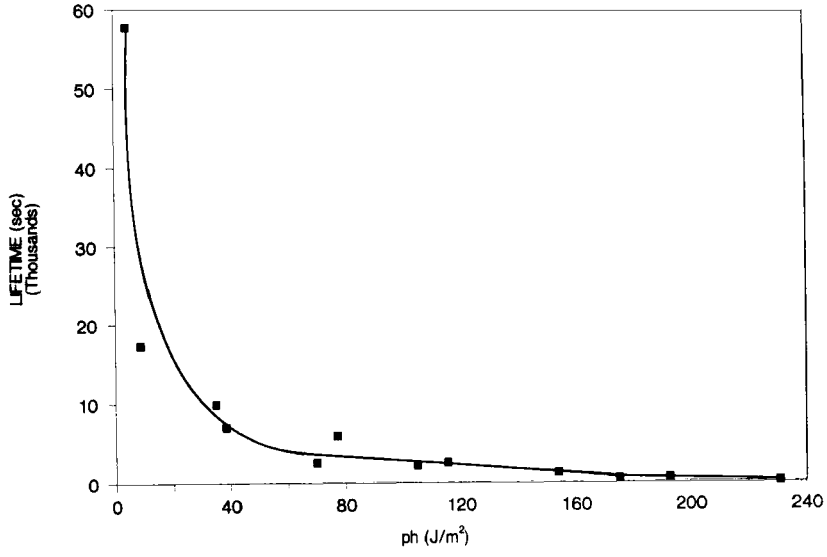

FIGURE 20 Lifetime *versus ph*.

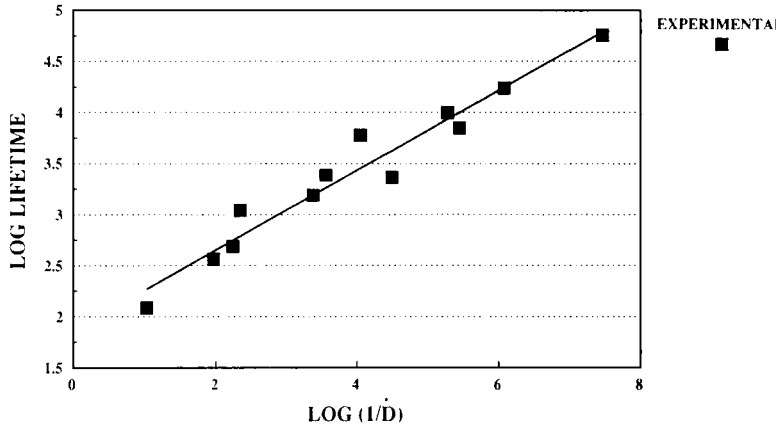

FIGURE 21 Log(lifetime) *versus* $\log(1/\dot{D})$.

experiments where film and test geometries are kept constant. Therefore, we relate changes in $\dot{D}$, as manifestation of changes in the rate of energy dissipation within the active zone. Inspecting $\dot{D}$, we observe that at high *ph*, the rate of energy dissipation increases. The increase in the rate of energy dissipation is related to the decrease in lifetime observed with increasing *ph*.

In our theoretical analysis, we derived a relationship correlating the rate of change in the detached area to the fracture energy, γ, and the rate of change in the energy dissipated within the active zone. In our proposed method for evaluating the rate of energy dissipation, we assumed that the energy dissipated is due solely to viscoelastic processes. Implicit in the derivation of the rate of energy dissipation is the proportionality between strain rate and strain *within the active zone.* Viscoelastic theory establishes a relationship between strain rate and strain of the form:

$$\dot{\varepsilon} = (1/t)\varepsilon \tag{2}$$

where t is the relaxation time. Although $\dot{D}$ is related to film properties, test geometry and dissipative factors, it is obvious from Eq. (2) that the dissipative component should be related to the inverse of $\dot{D}$. The inverse of $\dot{D}$ may then be suggested as a measure of the resistance of the adhesive bond to deformation. When the log of lifetime is plotted versus the log of $1/\dot{D}$, a linear relationship is observed (see Figure 21).

Dissipative coefficient, β

$\dot{D}$, the rate of energy dissipated in irreversible deformation processes in the active zone, is dependent on both material and geometric parameters. In an attempt to

separate the geometric and material factors, we have proposed a first order approximation to $\dot{D}$ of the form:[20]

$$\dot{D} = \beta p^2 h A(t) \tag{3}$$

where β is a phenomenological coefficient related to geometric and material parameters, p is the applied pressure, h is the constrained blister height and $A(t)$ is the blister area. Combining Eqs. (1) and (3), we arrive at a formalism relating time dependent blister growth and interfacial parameters, γ and β of the form:

$$\frac{A(t)}{A(t_0)} = \exp\left[\frac{\beta p^2 h}{ph - \gamma}(t - t_0)\right] \tag{4}$$

where $A(t)$ is the blister area at time t; p is the applied pressure; h is the constrained blister height; γ is the energy of interfacial adhesion; and β is a phenomenological coefficient related to material properties, geometrical factors and dissipative behavior.

Taking the natural log of Eq. (4), a linear relationship between time dependent detached area, $A(t)$, and interfacial parameters, γ and β, is obtained, *i.e.*,

$$\ln \frac{A(t)}{A(t_0)} = \frac{\beta p^2 h}{ph - \gamma}(t - t_0) \tag{5}$$

The plot of natural log of the normalized area $(A(t)/A(t_0))$ *versus* the reduced time is presented in Figure 22. Although a good fit to the data is obtained using this data reduction format, deviations from linearity are observed, possibly due to the first order assumptions made in deriving the dissipative component of the phenomenological coefficient, β.[15] From the slope of the lines presented in Figure

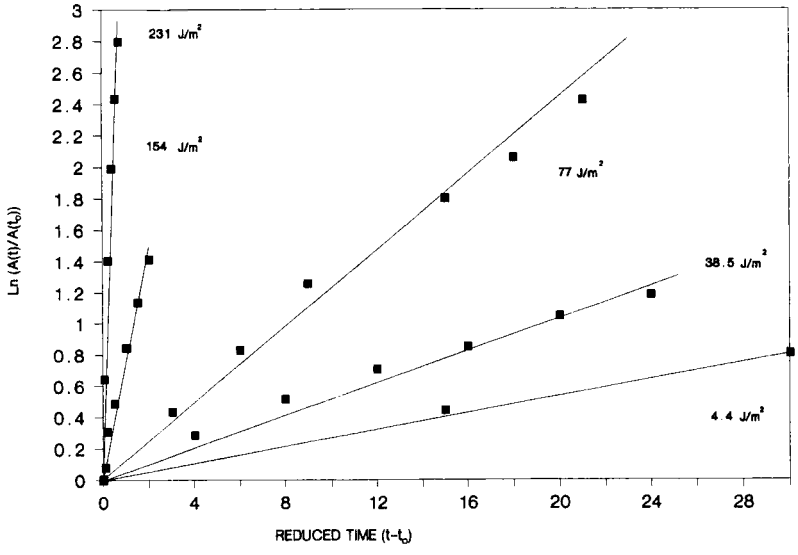

FIGURE 22 Ln$[A(t)/A(t_0)]$ *versus* reduced time, $t - t_0$.

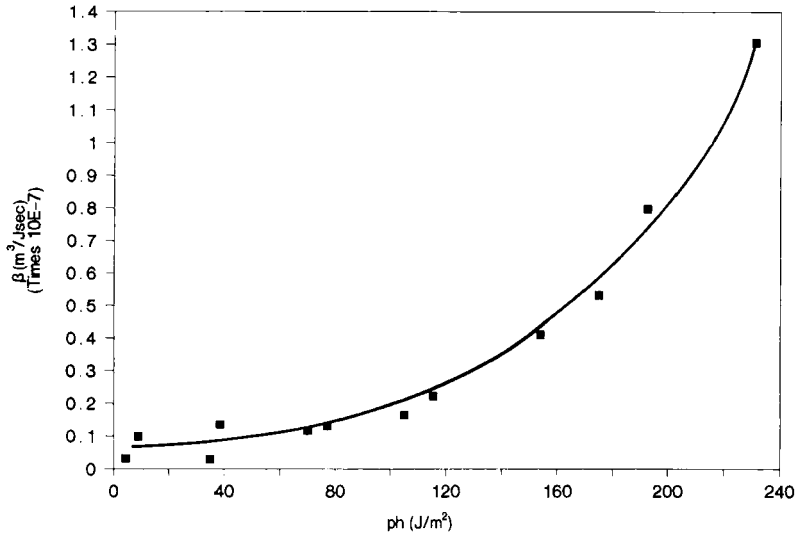

FIGURE 23 Phenomenological coefficient, β, *versus ph*.

22, the phenomenological coefficient β can be calculated using a value for γ of $1.8\,J/m^2$. The phenomenological coefficient β is presented in Figure 23 as a function of *ph*. A sharp increase in β is observed with increasing *ph*.

Analogous to the analysis used for $\dot{D}$, we plot the log $(1/\beta)$ *versus* the log of lifetime and observe a linear relationship (see Figure 24). The similar dependence of lifetime on the reciprocals of both $\dot{D}$ and β reinforces our belief that the assumptions made in deriving β are valid.

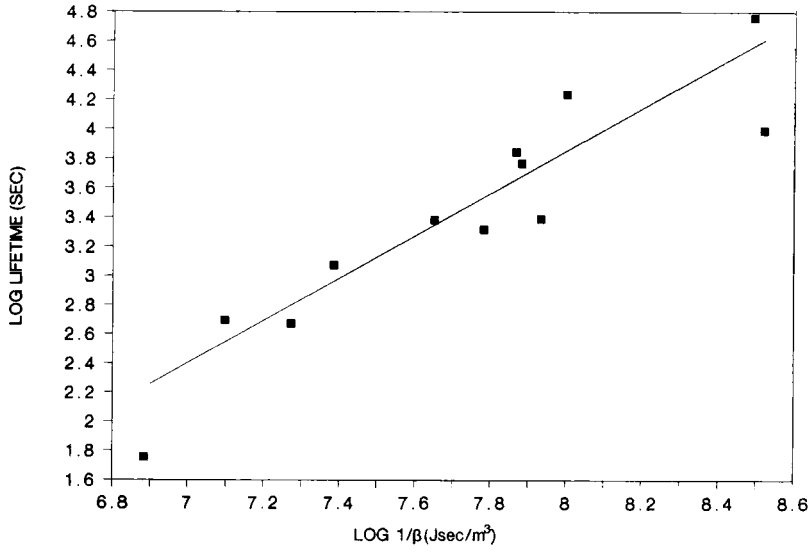

FIGURE 24 Log(lifetime) *versus* $\log(1/\beta)$.

Although $\dot{D}$ and β contain film and geometric factors, this finding suggests a fundamental direction to quantifying the lifetime of an interface. However, it should be stressed that these conclusions are based on a single experimental study of one type of adhesive tape. The applicability of our approach and utility of β in predicting lifetime outside of this constrained blister geometry needs to be verified with further experimental study.

CONCLUSIONS

A detailed investigation of the failure behavior of a pressure sensitive adhesive tape was performed utilizing the constrained blister test. An energy of interfacial adhesion of $1.8\,J/m^2$ was determined for the PSA tape on a copper substrate. An active zone was visualized through the use of a tape with transparent backing. The deformation within the active zone was found to consist of cavitation and deformation of ligaments. Fracture of the ligaments caused the detachment front to advance. It has been proposed that $\dot{D}$ reflects the resistance of the adhesive bond to time dependent deformation. A relationship was established between lifetime and the inverse of the rate of energy dissipated in the active zone.

Acknowledgement

The authors wish to thank the Center for Adhesives, Sealants and Coatings at Case Western Reserve University for financial support during the course of this work.

References

1. D. L. Hunston, A. J. Kinloch, and S. S. Wang, *J. Adhension*, **28,** 103 (1989).
2. S. Wu, *Polymer Interface and Adhesion*, (Marcel Dekker Inc., N.Y., N.Y., 1982).
3. I. Skeist, Ed., *Handbook of Adhesives, -3rd Ed.*, (Van Nostrand Reinhold, N.Y., 1989).
4. A. J. Kinloch, *Adhesion and Adhesives—Science and Technology*, Chapman & Hall, N.Y., 1987).
5. W. S. Johnson, Ed., *Adhesively Bonded Joints: Testing, Analysis and Design*, **STP 981,** (ASTM 1988).
6. K. Kim and J. Kim, *Trans. ASME*, WA/EEP-3 (1986).
7. H. Dannenberg, *J. Appl. Polym. Sci.*, **5,** 125 (1961).
8. M. L. Williams, *J. Appl. Polym. Sci.*, **13,** 29 (1969).
9. M. L. Williams, *J. Appl. Polym. Sci.*, **14,** 1121 (1970).
10. J. D. Burton and W. B. Jones, *Trans. Soc. Rheol.*, **15,** (1), 39 (1971).
11. M. L. Williams, *J. Adhesion*, **4,** 307 (1972).
12. S. J. Bennett, K. L. DeVries and M. L. Williams, *Int. J. of Fracture*, **10,** (1), 33 (1974).
13. J. A. Hincley, *J. Adhesion*, **16,** 115 (1983).
14. M. Allen and S. Senturia, in *Proceedings of the ACS, Div. of Polym. Mater. Sci. and Eng.*, **56,** 735 (1987).
15. A. N. Gent and L. H. Lewandowski, *J. Appl. Polym. Sci.*, **33,** 1567 (1987).
16. A. N. Gent and R. P. Petrich, *Proc. Royal Soc.*, **A310,** 433 (1969).
17. E. Orowan, *J. Franklin Instit.*, **290,** 493 (1970).
18. A. N. Gent and A. J. Kinloch, *J. Polym. Sci., A-2*, **9,** 659 (1971).
19. M. J. Napolitano, A. Chudnovsky and A. Moet, in *Proceedings of the ACS, Div. of Polymer Sci. and Eng.*, **57,** 755 (1987).
20. M. J. Napolitano, A. Chudnovsky and A. Moet, *J. Adhesion Sci. & Techn.*, **2,** (4), 311 (1988).
21. Y.-S. Chang, Y.-H. Lai and D. A. Dillard, *J. Adhesion*, **27,** 197 (1989).

22. Y. H. Kim, G. F. Walker, J. Kim and J. Parker, *J. Adhesion Sci. & Techn.*, **1,** (4), 331 (1987).
23. D. H. Kaeble, *Trans. Soc. Rheol.*, **9,** (2), 135 (1965).
24. D. H. Kaeble, *J. Adhesion,* **1,** 102 (1969).
25. D. H. Kaeble and R. S. Reylek, *J. Adhesion,* **11,** 124 (1969).
26. Y. Urahama, *J. Adhesion,* **31,** 47 (1989).
27. G. H. Lindsey, *J. Appl. Phys.*, **38,** (12), 4843 (1967).